Available online at www.sciencedirect.com
ScienceDirect
Trans. Nonferrous Met. Soc. China 25(2015) 2081−2086
Transactions of Nonferrous Metals Society of China
www.tnmsc.cn

Hydrothermal synthesis of silver nanoparticles in Arabic gum aqueous solutions

Ying-fen LI, Wei-ping GAN, Jian ZHOU, Zhi-qiang LU, Chao YANG, Tian-tian GE

School of Materials Science and Engineering, Central South University, Changsha 410083, China

Received 25 June 2014; accepted 25 March 2015

Abstract: Finely divided silver nanoparticles were synthesized via the hydrothermal method. Arabic gum (AG) was used as both the reductant and steric stabilizer without any other surfactant. By adjusting the reaction temperature, mass ratio of AG to $AgNO_3$, and reaction time, silver nanoparticles with different morphological characteristics could be obtained. The products were characterized by UV−Vis, FTIR, TEM, SEM, and XRD measurements. It was found that temperature and AG played an important role in the synthesis of mono-disperse silver nanoparticles. Well dispersed and quasispherical silver nanoparticles were obtained under the optimal synthesis conditions of 10 mmol/L $AgNO_3$, m(AG)/m($AgNO_3$)=1:1, 160 °C and 3 h.

Key words: silver nanoparticles; hydrothermal method; Arabic gum; green chemistry

1 Introduction

Recently, silver nanoparticles have been widely used in optical devices, catalysts, biologic nanosensors, photonic crystals, and electronics due to their fascinating optical, electrical, catalytic and thermal properties [1−4]. Therefore, it is necessary to develop a simple procedure with optimized conditions to synthesize uniform silver nanoparticles.

Several strategies have been developed for synthesizing silver particles: wet chemical reduction [5], photo-chemical reduction [6], sonochemical method [7], and hydrothermal method [8]. Most of the above strategies involve the reduction of $AgNO_3$ with a reducing agent, such as sodium sulfite, hydrazine, and iron (II) sulfate, in the presence of a suitable protecting agent [8−10]. However, many reducing and protecting agents pose potential environmental and biological risks. With the growing concerns on the biological and environmental impact of nanomaterials, green synthesis of silver nanoparticles has recently become one of the study hot spots [1,5,11]. YANG and PAN [1] fabricated silver nanoparticles with sodium alginate as both reducing and stabilizing agents via the hydrothermal method [1]. DADOSH [5] prepared uniform silver nanoparticles with a controllable size with tannin as the reducing agent. PHILIP [11] reported the green synthesis of silver nanoparticles with honey as reducing and stabilizing agents.

Arabic gum (AG) is a complex polysaccharide, which is obtained as sticky exudates from the stems and branches of Acacia trees [12,13]. It is an excellent dispersant in the preparation of silver microspheres and can endow silver powder with dispersibility. However, $AgNO_3$ was reduced by ascorbic acid in these synthesis routes [14,15]. As the main components of AG, polysaccharides (galactosyl, arabinosyl, rhamnosyl, glucuronosyl, and 4-O-methyl-glucuronosyl), are effective reducing agents [13,16], we employed AG as both the reducing agent and the dispersant in this work. $AgNO_3$ was directly reduced to silver nanoparticles by AG via the hydrothermal method without any other surfactant.

2 Experimental

2.1 Preparation of silver nanoparticles

All the chemicals were of analytical grade and purchased from Shanghai Chemical Reagent Company, China, for direct use without further purification. In a typical process, 0.5 mmol/L $AgNO_3$ and 0.1 g AG were dissolved into 50 mL of deionized water in a 100 mL Teflon vessel. Then, the resulting mixture was sealed in a stainless steel autoclave and maintained at 160 °C for 3 h. After the reaction was completed, the autoclave was cooled down to room temperature naturally. The products were collected by centrifugation and washed

Corresponding author: Wei-ping GAN; Tel: + 86-13707311733; E-mail: gwp@mail.csu.edu.cn
DOI: 10.1016/S1003-6326(15)63818-3

with water and ethanol five times, respectively. Then, they were dispersed in ethanol for further characterization.

2.2 Characterization

The UV−Vis spectra of aqueous solutions were measured by an UV−Vis spectrophotometer (Rayleigh UV−1801). The morphology of silver nanoparticles was observed by TEM (FEI Tecnai−G2−20ST). The morphology of carbon spheres was observed by SEM (MIRA3 TESCAN). The phase structure of the sample was examined by X-ray diffraction (D−MAX2500). The FTIR spectra of silver nanoparticles were recorded on an FTIR spectrometer (Nicolet 6700).

3 Results and discussion

3.1 UV−Vis spectra of silver nanoparticles

Silver nanoparticles exhibit different UV−Vis absorption peaks depending on their shapes and sizes [1,2]. Figure 1 shows the UV−Vis absorption spectra of products in the aqueous solution synthesized at different temperatures ($c(Ag^+)$=10 mmol/L, R (mass ratio of AG to $AgNO_3$)=1:1, t=3 h). With the increase in temperature, the intensity of absorption band increases firstly and then decreases. When the temperature increases from 120 to 160 °C, the peak intensity is enhanced with blue shifts from 430 to 425 nm, indicating that the content of silver nanoparticles increases while the particle size decreases with the increase of the temperature. The absorption peak of 425−430 nm is assigned to the out-of-plane dipole resonance of silver nanoparticles [17]. However, it is hard to observe the peak of silver nanoparticles because its intensity decreases and the absorption band is broadened at 180 °C due to the longitudinal plasmon resulting from the aggregation of silver particles [18]. Similar phenomenon was observed by WANG et al [8] in the preparation of silver nanoparticles with $[AgSO_3]^-$ and PVP [8]. AG polysaccharides are made of monosaccharide, such as galactose, arabinose, and rhamnose [12,13]. It can be easily carbonized at high temperatures, especially when they are mixed with metal ions. Therefore, the aggregation of silver nanoparticles is ascribed to the carbonization of AG. These phenomena will be confirmed in Section 3.4.

AG polymer chains contain lots of charged groups (—COOH and —NH_2), which can coordinate with Ag^+ to form complex compounds (Ag^+−AG) [15]. Moreover, the C—C bonds of polysaccharides can be easily cleaved to release electrons required for the reduction of Ag^+ at high temperatures [16]. When the complex compound Ag^+−AG is reduced to Ag^0−AG, AG polymer chains endow silver nanoparticles with excellent dispersibility through the steric effect. Figure 2 shows the UV−Vis spectra of silver nanoparticles prepared at different R values (160 °C, 3 h, $c(Ag^+)$=10 mmol/L). R was found to exhibit important influence on the reduction efficiency of Ag^+ and the particle size distribution of nanoparticles. Although a small R is enough to reduce Ag^+ to silver nanoparticles, the absorption peak is so weak, indicating that AG is insufficient. In addition, the absorption band at a small R is broadened. It is well known that the UV−Vis absorption band of silver nanoparticles is related to their particle size distribution. The absorption band becomes broad when silver nanoparticles have a wide particle size distribution. Similar to other steric stabilizing agents, such as PVP and sodium citrate [8,10], the increase of AG dosage can intensify its steric effect. As R increases, the plasmon absorption peak is blue-shifted from 438 to 425 nm and the absorption bands become narrow, indicating that the particle size decreases and particle size distribution becomes narrow as R increases. The peak nearly reaches the maximum absorption intensity when R is 1:1, indicating that the R

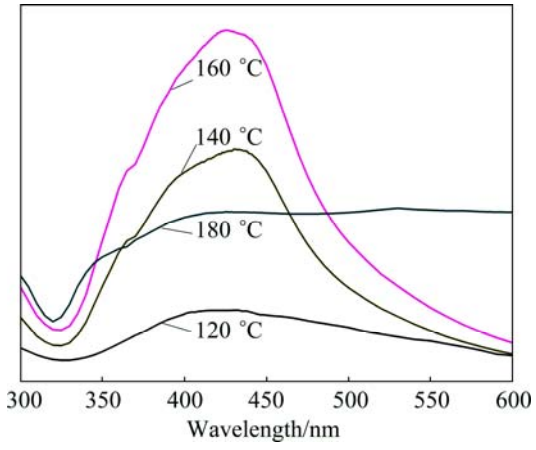

Fig. 1 UV−Vis absorption spectra of silver nanoparticles obtained at various temperatures ($c(Ag^+)$=10 mmol/L, R=1:1, t=3 h)

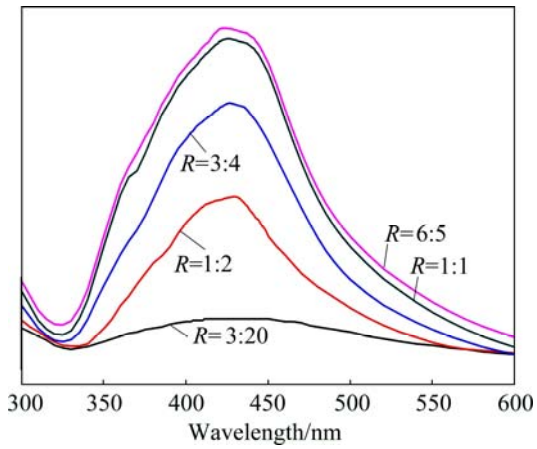

Fig. 2 UV−Vis absorption spectra of Ag nanoparticles obtained at various R values (160 °C, 3 h, $c(Ag^+)$=10 mmol/L)

of 1:1 can ensure the complete reduction of Ag^+. When R is 6:5, the peak is blue-shifted further, but its absorbance is almost identical to that obtained at the R of 1:1.

The formation of silver nanoparticles involves two steps: nucleation and growth. In order to understand the evolution process of silver nanoparticles, we obtained the UV−Vis absorption spectra of silver nanoparticles prepared at different time (160 °C, $c(Ag^+)$=10 mmol/L, R=1:1). As shown in Fig. 3, silver nanoparticles are formed after 0.5 h. The peak of silver nanoparticles is centered at 411 nm with a narrow absorption band, but the absorption intensity is so weak. As the reaction proceeds, the intensity of absorption peak of silver nanoparticles is enhanced. The major plasmon peak is red-shifted and reaches a final wavelength value of 425 nm after 3 h. The shift of the maximum wavelength of the absorption spectrum during the reaction is similar to previous reports [9]. However, the absorption bands are not changed obviously, indicating that the particle size gradually becomes large in the reaction, but particle size distribution is not changed markedly.

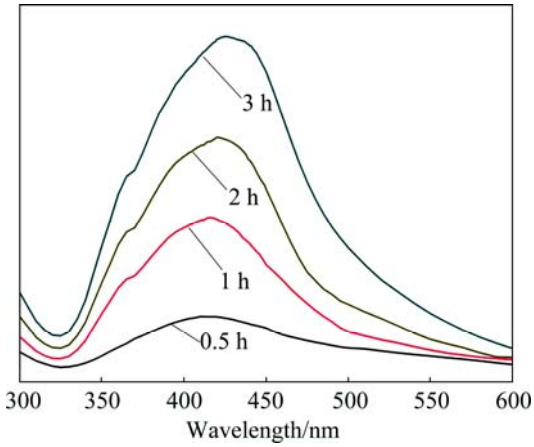

Fig. 3 UV-Vis absorption spectra of silver nanoparticles obtained at various reaction time (160 °C, $c(Ag^+)$=10 mmol/L, R=1:1)

3.2 Morphology of silver nanoparticles

The typical TEM images of silver nanoparticles obtained in this work are shown in Fig. 4. The products obtained at 140 °C (Fig. 4(a)) and 160 °C (Fig. 4(b)) are well dispersed, quasispherical in shape, and coated by AG. The mean particle size decreases from 24 nm to 18 nm when the temperature is increased from 140 °C to 160 °C. The silver nanoparticles prepared at 140 °C consist of large and small particles ranging from 10 to 50 nm, while the sizes of the products obtained at

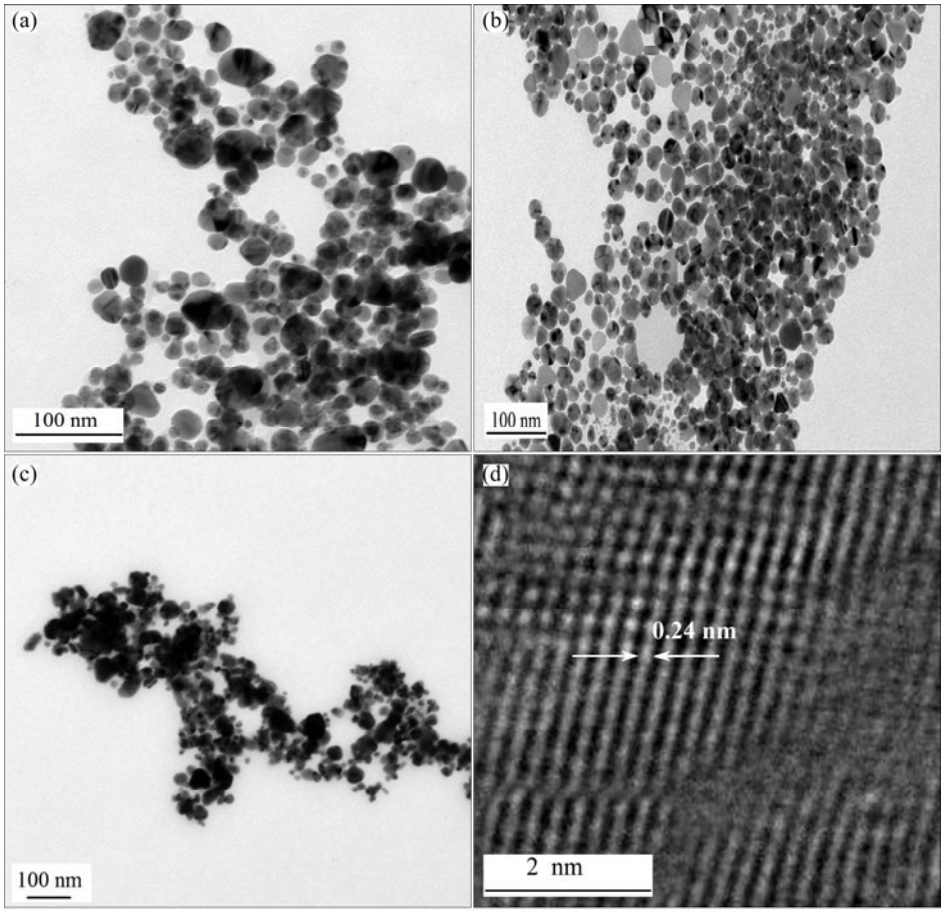

Fig. 4 TEM images of silver nanoparticles prepared at different temperatures ($c(Ag^+)$=10 mmol/L, R=1:1, t=3 h): (a) 140 °C; (b) 160 °C; (c) 180 °C; (d) Typical HRTEM image of silver nanopaticle shown in (b)

160 °C range from 15 to 25 nm. At low temperatures, the nucleation rate is similar to the growth rate. The particles formed initially act as the seeds and become larger as reaction proceeds. At the same time, other small nanoparticles are formed. A moderately elevated temperature is conductive to the fast nucleation. In addition, when the nucleation rate is larger than growth rate, small particles with a narrow size distribution can be easily obtained. On the contrary, the products obtained at 180 °C (Fig. 4(c)) are severe aggregates, which is consistent with the results of UV−Vis spectra (Fig. 1). Moreover, AG coated on the particle surface nearly disappears completely, which is the reason for the agglomeration. Without enough dispersant, the silver nanoparticles cannot be well dispersed. The reason will be discussed below. Figure 4(d) shows the HRTEM image of a typical particle from Fig. 4(b). Obviously, a lattice spacing of 0.24 nm corresponding to the (111) plane of Ag is observed, indicating that the growth of Ag nanoparticles occurs preferentially on the plane (111) [8,11].

The color of reaction solutions is related to the size, content, and morphology of Ag nanoparticles [1,2,5−8]. The color is changed from yellow at 120 °C, brown at 140 °C, to reddish-brown at 160 °C and light yellow with dark precipitate at 180 °C (Fig. 5). According to the TEM images of silver nanoparticles and the results of UV−Vis spectra, the silver nanoparticle solutions with well-dispersed spherical nanoparticles smaller than 50 nm are yellow. With the increase in the nanoparticle content, the color of the solutions turns to be reddish-brown. When most of the nanoparticles become aggregates, they are deposited at the bottom of the beaker and the solution turns light yellow.

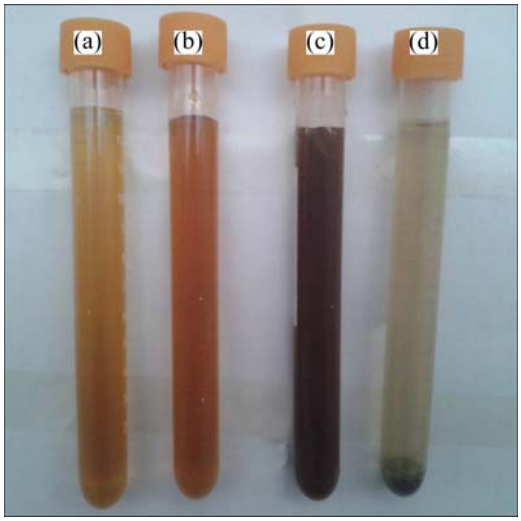

Fig. 5 Photographs of as-prepared Ag nanoparticle solutions prepared at different temperatures ($c(Ag^+)$=10 mmol/L, R=1:1, t=3 h): (a) 120 °C; (b) 140 °C; (c) 160 °C; (d) 180 °C

3.3 FTIR spectra of silver nanoparticles

Figure 6 shows the FTIR spectra of different silver nanoparticles prepared at 160 °C and 180 °C, respectively. In the spectrum of the products obtained at 160 °C, the main characteristic peaks of —COOH groups of Arabic gum can be observed at 1072 and 1421 cm^{-1} (C — O stretching), 1618 cm^{-1} (C═O stretching), 2925 cm^{-1} (C—H stretching), and 3425 cm^{-1} (O—H stretching), indicating that AG acting as a steric stabilizing agent is adsorbed on the particle surface to prevent the aggregation of silver nanoparticles. In the spectrum of the nanoparticles obtained at 180 °C, only the characteristic peak of —OH at 3428 cm^{-1} can be observed clearly. Moreover, its intensity is much smaller than that of the nanoparticles obtained at 160 °C. The peaks of C—O and C═O stretching are too weak to be observed, indicating that a little AG covers the particle surface and results in the agglomeration of nanoparticles. Because the steric effect is largely determined by the covering fraction of AG on the particle surface, it is required to coat the nanoparticles fully with enough AG in order to obtain finely-divided nanoparticles. At high temperatures (≥180 °C), the majority of carbohydrates can be carbonized, especially when they are mixed with metal ions [19−21]. For example, regular carbon spheres can be synthesized via a simple glucose hydrothermal process at 180 °C [22]. The decrease in the covering fraction of AG on the particle surface in this study may result from the carbonization of AG.

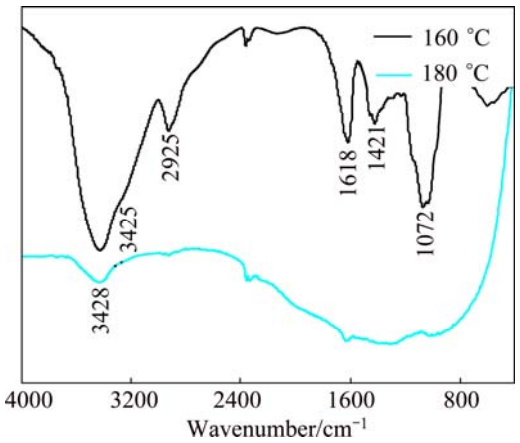

Fig. 6 FTIR absorption spectra of silver nanoparticles obtained at different reaction temperatures ($c(Ag^+)$=10 mmol/L, R=1:1, t=3 h)

3.4 Reference experiment

Saccharides, such as glucose and starch, are usually used as starting materials in the synthesis of carbon materials [21,22]. Because AG contains lots of polysaccharides, it can be carbonized via a hydrothermal carbonization process. As a reference experiment, 2 g/L AG aqueous solution was hydrothermally treated at

180 °C respectively for 6 and 12 h. As shown in Fig. 7(a), the products treated for 6 h are spherical particles with tough surfaces. Moreover, the particles are connected with each other, indicating that carbon spheres are formed at that moment. As the reaction proceeds, the larger particles with smooth surfaces are obtained after 12 h (Fig. 7(b)). Although carbon spheres could not be obtained after 3 h (Fig. 4(c)), similar to starch, AG started to be hydrolyzed to produce monosaccharides [21]. Furthermore, Ag^+ acted as a catalyst to accelerate the carbonization of AG when $AgNO_3$ was mixed with AG [19,20]. Then, AG polymer chains were shortened and the steric effect of AG was greatly reduced. Therefore, the aggregates of silver nanoparticles were obtained.

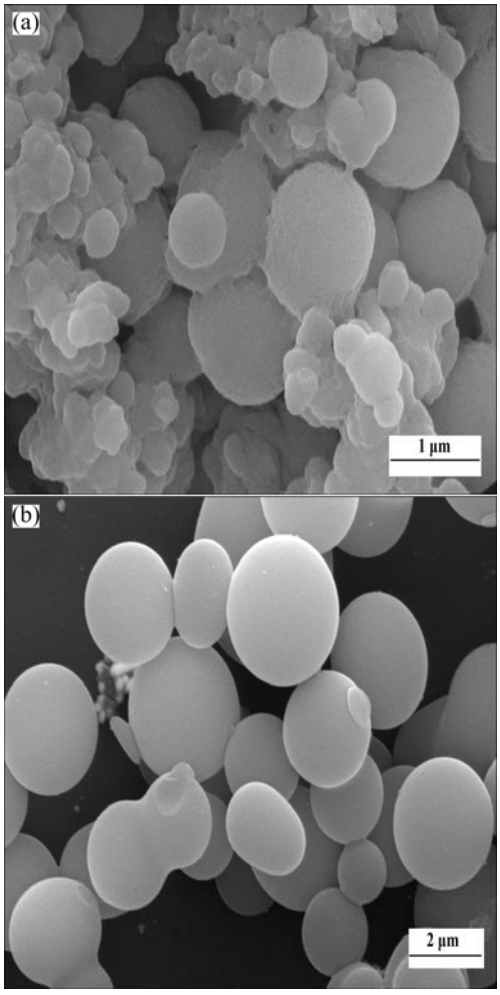

Fig. 7 SEM images of carbon spheres prepared with 2 g/L Arabic gum at 180 °C for different time: (a) 6 h; (b) 12 h

3.5 XRD patterns of products

Figure 8 presents the XRD patterns of silver nanoparticles and carbon spheres. The diffraction peaks (Fig. 8(a)) at 38.5°, 44.6°, 64.5°, and 78.2° respectively correspond to (111), (200), (220), and (311) lattice planes of silver nanoparticles. All these diffraction peaks are matched to the face-centered cubic (FCC) crystal structure of silver. The cell parameter is calculated to be 4.086 Å, which is close to the reference value (JCPDS No. 04−0783). As shown in Fig. 8(b), only the weak reflection peak of (002) plane is observed, indicating that carbon spheres are in the amorphous carbon phase.

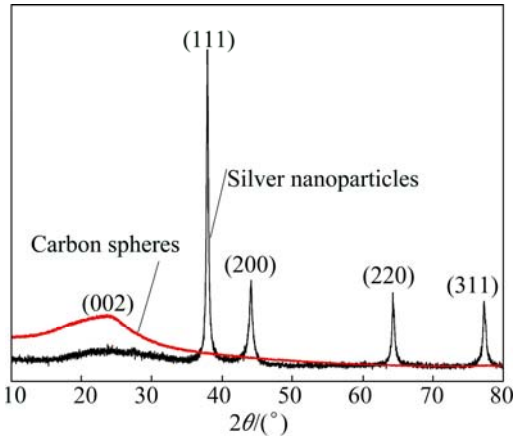

Fig. 8 XRD patterns of silver nanoparticles and carbon spheres

4 Conclusions

1) Well dispersed silver nanoparticles with a narrow size distribution were prepared by reducing $AgNO_3$ with AG via the hydrothermal method.

2) AG acts as both the reductant and steric stabilizer. Polysaccharides in AG act as the reductant, and AG polymer chains endow silver nanoparticles with excellent dispersibility through the steric effect.

3) AG can be carbonized under moderate reaction conditions, thus endowing silver nanoparticles with poor dispersion.

References

[1] YANG J S, PAN J. Hydrothermal synthesis of silver nanoparticles by sodium alginate and their applications in surface-enhanced Raman scattering and catalysis [J]. Acta Materialia, 2012, 60(12): 4753−4758.

[2] YI Zao, ZHANG Jian-bo, HE Hua, XU Xi-bin, LUO Bing-chi, LI Xi-bo, LI Kai, NIU Gao, TAN Xiu-lan, LUO Jing-shan, TANG Yong-jian, WU Wei-dong, YI You-gen. Convenient synthesis of silver nanoplates with adjustable size through seed mediated growth approach [J]. Transactions of Nonferrous Metals Society of China, 2012, 22(4): 865−872.

[3] YI Zao, ZHANG Jian-bo, CHEN Yan, CHEN Shan-jun, LUO Jian-shan, TANG Yong-jian, WU Wei-dong, YI You-gen. Triangular Au−Ag framework nanostructures prepared by multi-stage replacement and their spectral properties [J]. Transactions of Nonferrous Metals Society of China, 2011, 21(9): 2049−2055.

[4] PARK J K, SEO D S, LEE J K. Conductivity of silver paste prepared from nanoparticles [J]. Colloids and Surfaces A: Physicochem Eng Aspects, 2008, 313−314: 351−354.

[5] DADOSH T. Synthesis of uniform silver nanoparticles with a controllable size [J]. Materials Letters, 2009, 63(26): 2236−2238.

[6] STAMPLECOSKIE K G, SCAIANO J C. Light emitting diode

irradiation can control the morphology and optical properties of silver nanoparticles [J]. Journal of American Chemical Society, 2010, 132(6): 1825−1827.
[7] TALEBI J, HALLADJ R, ASKARY R. Sonochemical synthesis of silver nanoparticles in Y-zeolite substrate [J]. Journal of Materials Science, 2010, 45(12): 3318−3324.
[8] WANG X, LIN Y, GU F, LIANG Z, DING X F. A facile route to well-dispersed single-crystal silver nanoparticles from $[AgSO_3]^-$ in water [J]. Journal of Alloys and Compounds, 2011, 509(27): 7515−7518.
[9] ZHANG Z T, ZHAO B, HU L M. PVP protective mechanism of ultrafine silver powder synthesized by chemical reduction processes [J]. Journal of Solid State Chemistry, 1996, 121(1): 105−110.
[10] ZHAI Ai-xia, CAI Xiong-hui, JIANG Xiao-ye, FAN Guo-zhi. A novel and facile wet-chemical method for synthesis of silver microwires [J]. Transactions of Nonferrous Metals Society of China, 2012, 22(4): 943−948.
[11] PHILIP D. Honey mediated green synthesis of silver nanoparticles [J]. Spectrochimica Acta, 2010, 75(3): 1078−1081.
[12] RENARD D, GARNIER C, LAPP A, SCHMITT C, SANCHEZ C. Structure of arabinogalactan-protein from Acacia gum: From porous ellipsoids to supramolecular architectures [J]. Carbohydrate Polymers, 2012, 90(1): 322−332.
[13] IDRIS O H M, WILLIAMS P A, PHILLIPS G O. Characterization of gum from Acacia senagal trees of different age and location using mutidetection gel permeation chromatography [J]. Food Hydrocolloid, 1998, 12(4): 379−388.
[14] LIU Z, QI X L, WANG H. Synthesis and characterization of spherical and mono-disperse micro-silver powder used for silicon solar cell electronic paste [J]. Advanced Powder Technology, 2012, 23(2): 250−255.
[15] LI Y F, GAN W P, LIU X G, LIN T, HUANG B. Dispersion mechanisms of Arabic gum in the preparation of ultrafine silver powder [J]. Korean Journal of Chemical Engineering, 2014, 31(8): 1490−1495.
[16] BALANTRAPU K, GOIA D V. Silver nanoparticles for printable electronics and biological applications [J]. Journal of Materials Research, 2009, 24(9): 2828−2836.
[17] JIN R C, CAO Y C, HAO E, METRAUXL G S, SCHATZ G C, MIRKIN C A. Controlling anisotropic nanoparticle growth through plasmon excitation [J]. Nature, 2003, 425: 487−490.
[18] ZHANG J, ROLL D, GEDDES C D, LAKOWICZ J R. Aggregation of silver nanoparticle−dextran adducts with concanavalin A and competitive complexation with glucose [J]. Journal of Physical Chemistry B, 2004, 108(32): 12210−12214.
[19] FANG Z, TANG K B, LEI S J, LI T W. CTAB-assisted hydrothermal synthesis of Ag/C nanostructures [J]. Nanotechnology, 2006, 17(12): 3008−3011.
[20] TITIRICI M M, ANTONIETTI M. Chemistry and materials options of sustainable carbon materials made by hydrothermal carbonization [J]. Chemical Society Reviews, 2010, 39: 103−116.
[21] ZHENG M T, LIU Y L, JIANG K M, XIAO Y, YUAN D S. Alcohol-assisted hydrothermal carbonization to fabricate spheroidal carbons with a tunable shape and aspect ratio [J]. Carbon, 2010, 48(4): 1224−1233.
[22] LI M, LI W, LIU S X. Control of the morphology and chemical properties of carbon spheres prepared from glucose by a hydrothermal method [J]. Journal of Materials Research, 2012, 27(8): 1117−1123.

阿拉伯树胶水热法制备银纳米颗粒

黎应芬，甘卫平，周 健，鲁志强，杨 超，戈田田

中南大学 材料科学与工程学院，长沙 410083

摘 要：在无其他表面活性剂的条件下，以阿拉伯树胶作为还原剂和位阻稳定剂，应用水热法制备具有良好分散性的银纳米颗粒。通过调节反应温度、阿拉伯树胶与硝酸银的质量比和反应时间，可以得到不同形貌的银纳米颗粒；采用 UV-Vis、FTIR、TEM、SEM 和 XRD 对反应所得产物进行表征。结果表明，反应温度和阿拉伯树胶在制备单分散银纳米颗粒过程中起重要作用；当硝酸银浓度为 10 mmol/L、阿拉伯树胶和硝酸银的质量比为 1:1、反应温度为 160 ℃、反应时间为 3 h 时，可以得到分散性良好的准球形银纳米颗粒。

关键词：银纳米颗粒；水热法；阿拉伯树胶；绿色化学

(Edited by Wei-ping CHEN)